

Experimental study of shear behavior of planar non-persistent joint

Hadi Haeri^{*1}, Vahab Sarfarazi² and Hossein Ali Lazemi³

¹*Department of Mining Engineering, Bafgh Branch, Islamic Azad University, Bafgh, Iran*

²*Department of Mining Engineering, Hamedan University of Technology, Hamedan, Iran*

³*Department of Mining Engineering, Bafgh Branch, Islamic Azad University, Bafgh, Iran*

(Received May 2, 2015, Revised January 5, 2016, Accepted February 13, 2016)

Abstract. The present article discusses the effect of the ratio of bridge surface to total shear surface, number of bridge areas and normal stress on the failure behavior of the planar non-persistent open joints. Totally, 38 models were prepared using plaster and dimensions of 15 cm×15 cm×15 cm. The bridge area occupied 45 cm², 90 cm² and 135 cm² out of the shear surface. The number of rock bridges increase in fixed area. Two similar samples were prepared on every variation in the rock bridges and tested for direct shear strength under two high and low normal loads. The results indicated that the failure pattern and the failure mechanism is mostly influenced by the ratio of bridge surface to total shear surface and normal stress so that the tensile failure mode change to shear failure mode by increasing in the value of introduced parameters. Furthermore, the shear strength and shear stiffness are closely related to the ratio of bridge surface to total shear surface, number of bridge areas and normal stress.

Keywords: bridge area; jointed specimen; crack propagation; indirect shear loading; shear-fracture behavior

1. Introduction

It is well known that the lower strength of rock mass is mainly induced by the presence of rock joints. In some rare cases, it is possible that the failure in the rock mass is limited to a single discontinuity. Generally, several discontinuities exist in various sizes, which constitute a combined shear surface. In this sense, the areas which are located between the neighboring discontinuities are called the Rock Bridges (see the definition in Fig. 1) and have the greatest importance for the shear resistance of the failure surface. (Eberhardt *et al.* 2002, Einstein *et al.* 1983, Janeiro and Einstein 2010, Jiang *et al.* 2014)

One claims to be on the safe side since the rock bridges are thought to produce a strength reserve, as they have to be broken first before failure can take place along the newly separated plane. Also, the coalescence of non-persistent joint causes rock failure in slopes, foundations and tunnels. Therefore, a comprehensive study on the shear failure behavior of jointed rock can provide a good understanding of both local and general rock instabilities, leading to an improved

*Corresponding author, Assistant Professor, E-mail: haerihadi@gmail.com



Fig. 1 (a) Rock bridges in discontinuously-jointed rock, (b) crack pattern in gypsum specimens in direct shear test



Fig. 2 (a) Cylindrical mold with 56 mm in diameter and 112 mm in length, (b) disc mold with 56 mm in diameter and 28 mm in thickness.

design for rock engineering projects.

Many experimental works have also been devoted to study the shear fracture of the pre-existing cracks in specimens of various substances, including natural rocks or concrete-like materials under various loading condition (Shen 1995, Wong *et al.* 2001, Sagong and Bobet 2002, Gehle and Kutter 2003, Mughieda and Khawaldeh 2004, 2006, Li *et al.* 2005, Barragán *et al.* 2006, Ayatollahi and Sistaninia 2011, Ozcebe 2011, Wang *et al.* 2011, Dai *et al.* 2011, Wang *et al.* 2012, Yoshihara 2013, Lancaster and Khalid 2013, Noël and Soudki 2014, Wang *et al.* 2015).

A common crack pattern found in rock-model materials in direct shear test was summarized by Ghazvinian *et al.* (2007) as follows (see Fig. 1a): 1. Wing cracks start at the tips of the fractures and propagate in a curvilinear path as the shear load increases. Wing cracks are tensile cracks, and they grow in a stable manner, since an increase in load is necessary to lengthen the cracks. Wing cracks tend to align with the direction of the shear stress. 2. Secondary cracks are generally described as shear cracks or shear zones. They initiate from the tips of the fractures.

Many studies have been carried out to determine the failure behavior of non-persistent joint (Gehle and Kutter 2003, Barragán *et al.* 2006, Ayatollahi and Sistaninia 2011). The novelty of this paper is to investigate the effect of the ratio of rock bridge surface to total shear surface, number of the Rock Bridge and normal stress on the failure behavior of open non-persistent rock joint. The sample size is chosen in such a way that provides an insight into the failure behavior in three dimensions.

In this article, the effect of the ratio of bridge surface to total shear surface, number of the bridge area and normal stress on the failure behavior of the open rock joint is studied. The sample size is chosen in such a way that provides an insight into the failure behavior in three dimensions.

2. Experimental studies

The discussion of experimental studies is divided into four sections. The first section discusses the physical properties of a modeling material, the second section is describing the technique of preparing the jointed specimens, the third section is focused on the testing procedure and finally, the fourth section considers the general experimental observations and discussions.

2.1 Modeling material and its physical properties

The material used for this investigation is gypsum, the same material was used by Shen *et al.* 1995; Bobet *et al.* (1998). Gypsum is chosen because, in addition to behave same as a weak rock, is an ideal model material which a wide range of brittle rocks can be represented; second, all the previous experiences and results can be incorporated and the earlier findings can be compared with the new ones; third, it allows to prepare a large number of specimens easily; Forth, repeatability of results. The samples are prepared from a mixture of the water and gypsum with a ratio of water to gypsum = 0.75. Concurrent with the preparation of specimens and their testing, uniaxial compression and indirect tensile strengths of the intact material was also tested in order to control the variability of material.

The uniaxial compressive strength (UCS) of the model material is measured on fabricated cylindrical specimens with 56 mm in diameter and 112 mm in length (Fig. 2a). The indirect tensile strength of the material is determined by the Brazilian test using fabricated solid discs 56 mm in diameter and 28 mm in thickness (Fig. 2b).

The testing procedure of uniaxial compressive strength test and the Brazilian test complies with the ASTM D2938-86 (1971) and ASTM C496-71 (1986), codes respectively.

The base material properties were obtained by authors is as follows

Average uniaxial compressive strength: 14 MPa

Average brazilian tensile strength: 1.2 MPa

Average Young's Modulus in compression: 3600 MPa

Average Poisson's ratio: 0.18

2.2 The technique in preparing the jointed specimens

The procedure developed by Bobet (1998) for preparing open non-persistent joints was used in this research with some modifications.

The material mixture is prepared by mixing water and gypsum in a blender; the mixture is then poured into a steel mold with internal dimension of 15×15×15 cm. The mold consists of four steel sheets bolted together and of two PMMA plates, 1/6 inch thick, which are placed at the top and bottom of the mold. As shown in Fig 3 the top plate has two rectangular openings used to fill the mold with the liquid gypsum mixture. The upper and the lower surfaces have slits cut into them. The width of slits is 0.5 mm (0.02 inch) and their length varies based on the length of the joints. The positions and number of the shims are predetermined to give a desired non-persistent joint.

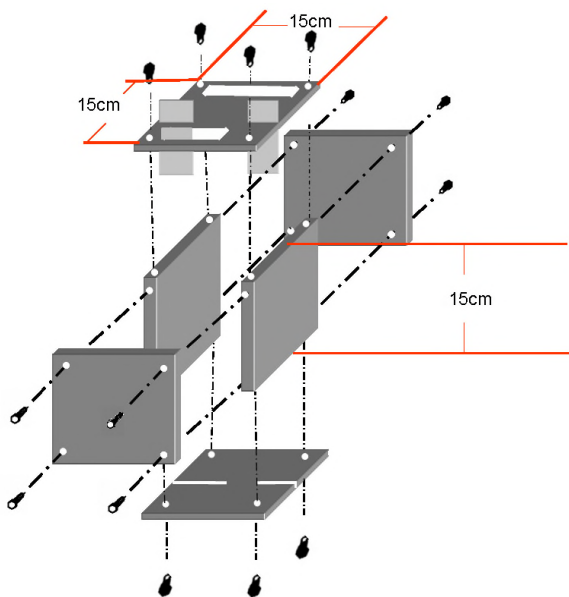


Fig. 3 Model used for the fabrication of the gypsum specimens

Table 1 The geometrical specifications of the various bridge areas

bridge sets	Shearing section	Bridge Area (cm ²)	a	b
	b	45	3	15
	b	90	6	15
	b a	135	9	15
	b a a			
	b a a a			

Through these slits, greased metallic shims are inserted through the thickness of the mold before pouring the gypsum. The mold with the fresh gypsum is vibrated and then stored at room temperature for 8 h afterward. The specimens un-molded and the metallic shims pulled out of the specimens; the grease on the shims prevents adhesion with the gypsum and facilitates the removal of the shims.

As the gypsum seated and hardened, each shim leaves in the specimen an open joint through the thickness and perpendicular to the front and back of the specimen. Immediately after removing the shims, the front and back faces of the specimens are polished and the specimen is stored in laboratory for 4 days. At the end of the curing process, the specimens are tested. It does not appear that the pull out of the shims produces any damage through the joints. The aperture of joints is 0.5 mm, therefore the joint surface has not any effect on the failure mechanism. The temperature of experimental room was 22°C.

The coplanar bridge areas have various configurations respect to shear loading direction and



Fig. 4 The physical models consisting non-persistent joints

Table 2 The amounts of the Effective non-persistent Joint Coefficients (EJC) for various configurations

bridge sets	Shearing section	Bridge Area		Total shear surface (TSS)	Effective joint coefficient (EJC=EJS/TSS)
		Effective Joint Surface (EJS)	Bridge Area		
	b b	45	225	0.8	
	a a	180			
	a a a	90	225	0.6	
	a a a	135			
	a a a	135	225	0.4	
	a a a	90			

have occupied 45 cm^2 , 90 cm^2 and 135 cm^2 of the total shear surface (225 cm^2) respectively. The geometry and dimensions of non-persistent joints has shown in Table 1. Also, the physical models have shown in Fig. 4.

Based on the change in the area of the bridge areas, it is possible to define the effective joint coefficient as the ratio of the effective joint surface (that is in front of the bridge areas) to the total

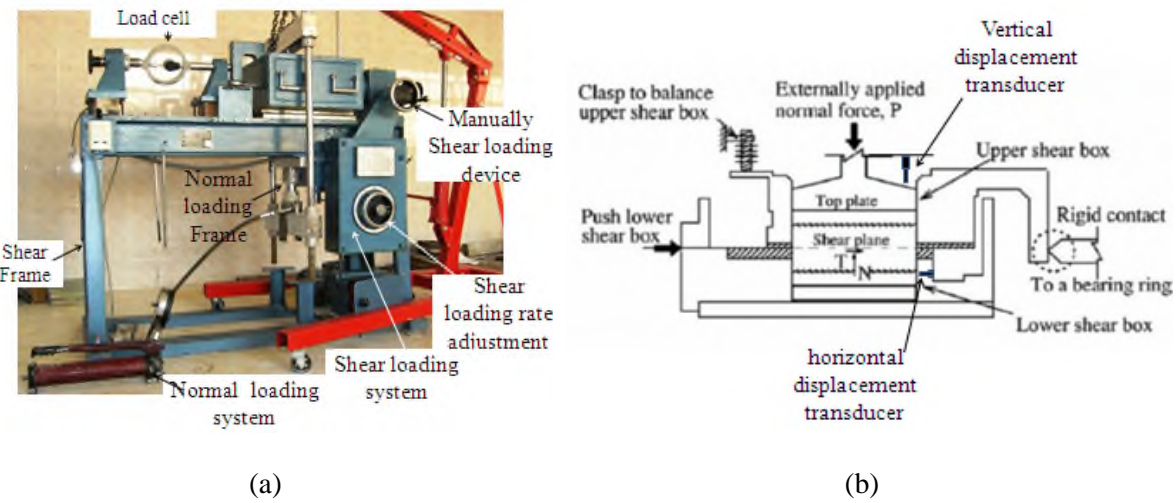


Fig. 5 Direct shear testing equipment, general set-up

shear surface (Takeuchi 1991, Haeri 2015).

In Table 2, the effective joint surface has shown as dotted area in front of the bridge area. Furthermore, the amount of the EJC is exhibited in this table. In order to study the complete failure behavior of bridge areas, two similar blocks were prepared and were tested under two different normal stresses (σ_n): 1 and 3.8 MPa.

Two identical specimens for each normal loading were prepared and tested to check repeatability. If the results from two identical tests show significant differences, a third specimen was prepared and tested.

2.3 Testing program

A total of 38 direct shear tests have been performed on specimens with discontinuous joints. All tests are displacement-controlled. The tests were performed in such a way that the normal load was applied to the sample and then shear load was adopted. Readings of shear loads, as well as the shear displacements are taken by a data acquisition system. Fig. 4 shows a schematic of the experimental set-up.

The conventional direct shear test apparatus, as shown in Fig. 5b, has both an upper and a lower shear boxes, and the sample is sheared along the plane between them by pushing the upper shear box horizontally with a normal (vertical) load applied to it. Normal loading is applied on the model using hydraulic jack (Fig. 5a). The normal load is registered using mechanical data acquisition system. Normal stress is measured by division of normal force to rock bridge area. Shear load can be applied in two ways; manually and or digitally. Shear loading was fixed in a rate of the 0.002 mm/s by using a shear loading rate adjustment system. According to the shear test standard method (Gehle and Kutter 2003), this loading rate is enough to establish the static condition during the test. The shear force is measured with a bearing ring or a load cell that is attached to the upper shear box.

Horizontal and vertical displacements were registered by displacement transducers installed in the right side and top of the box, respectively. The failure pattern was measured/observed after the

bridge area	Failure patterns in bridge areas with different number		
	One bridge area	Two bridge areas	Three bridge areas
RB Area = 45 cm^2			
RB Area = 90 cm^2			
RB Area = 135 cm^2			

Fig. 6 failure patterns in bridge areas under 8 MPa of normal stress

test was completed. The shearing process of a discontinuous joint constellation begins, as one would expect, with the formation of new fractures which eventually transect the material bridges and lead to a through-going discontinuity.

3. Observation

By observing the failure surface after the tests, it is possible to investigate the effect of bridge configurations (or EJC) and the normal stress on the failure mechanism of specimens. Fig. 6 shows the tested models at 3.8 MPa of normal stress and Figs. 7 and 8 summarizes the schematic of all observed crack patterns obtained in the direct shear tests.

The crack pattern is always a combination of only two types of cracks: wing cracks and shear cracks. Wing cracks start at the tip of the joints and propagate in a curvilinear path as the load increases. Wing cracks are tensile cracks and they grow in a stable manner, since an increase in load is necessary to lengthen the cracks. Shear cracks also initiate at tip of the joints and propagate in a stable manner.

3.1 The failure pattern in bridge areas under low normal stress

Latitudinal Rock Bridges Sets

The Failure Mode in the Introduced sections

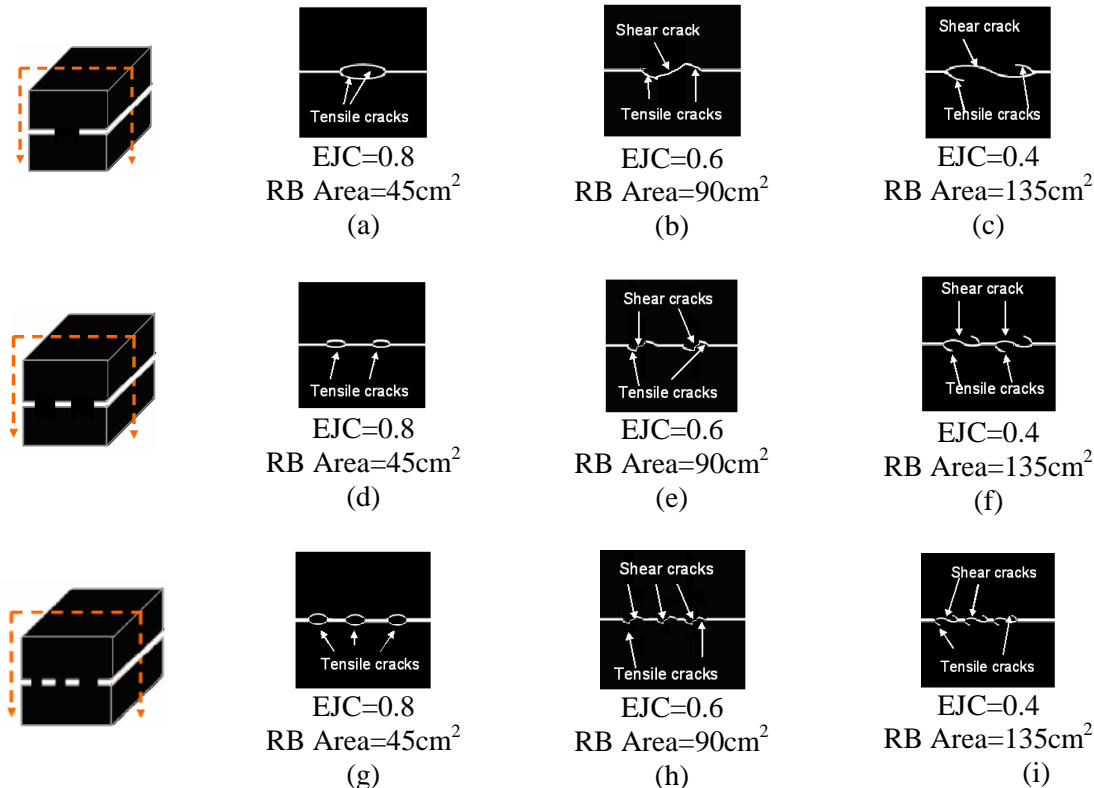


Fig. 7 The failure patterns in latitudinal rock bridge

Type I: The oval mode coalescence with two wing cracks

The oval mode coalescence, as defined in Fig. 7a, d and g, occurs when $\text{EJC}=0.8$. The wing cracks were initiated and propagated in curvilinear path that eventually aligned with the shear loading direction.

The wing cracks propagate in a stable manner; and the external load needs to be increased for the cracks to propagate further. Each wing crack was initiated at the tip of the one joint and finally coalesced with the tip of the other joint.

This coalescence left an oval core of intact material completely separated from the sample. The surface of failure is tensile because no crushed or pulverized materials and no evidence of shear movement were noticed. The wing cracks surfaces also had the same characteristics of tension surface. It is to be note that, when $\text{EJC}=0.8$ the oval mode coalescence appeared in samples consisting one, two and three bridge areas.

Type II: Coalescence with mixed crack (shear/tensile)

This coalescence, as defined in Fig. 7b, e and h occurred when $\text{EJC}=0.6$. At first the wing cracks were initiated at the tip of the joints and propagated stably. These wing cracks connect to each other by a shear crack.

Examining the failure surface in near the joint tips, it was noticed that there was smooth and

Latitudinal Rock Bridges Sets

The Failure Mode in the Introduced sections

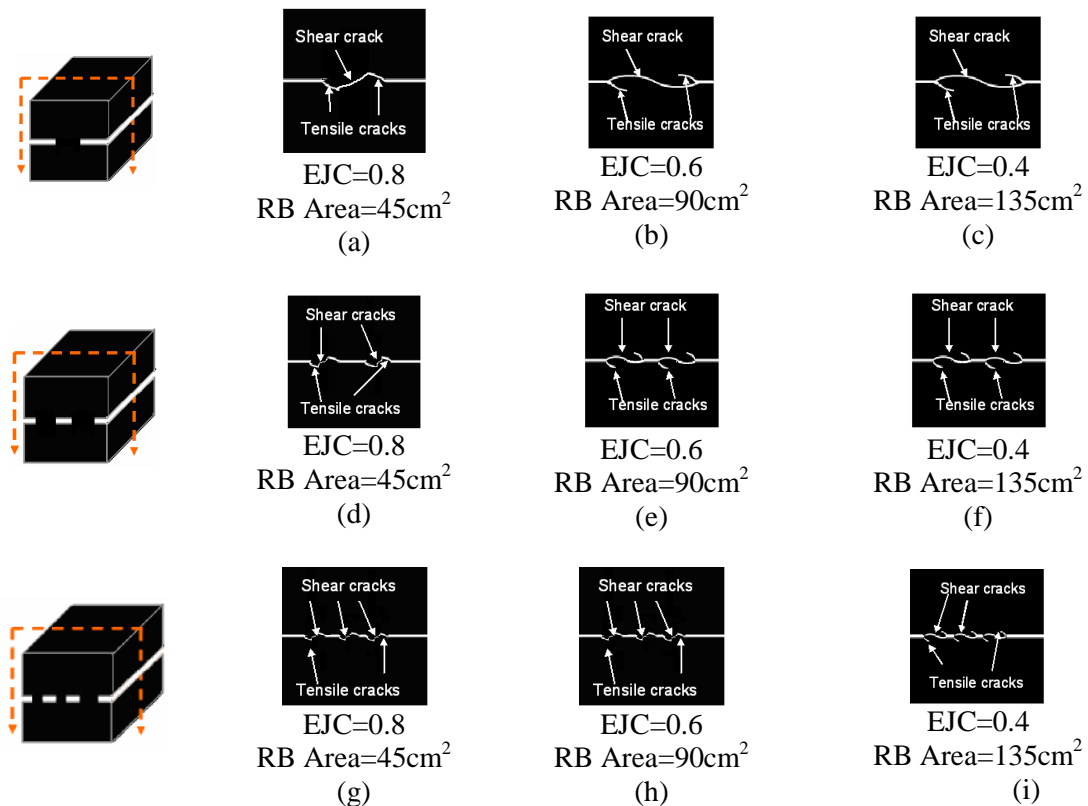


Fig. 8 The failure patterns in latitudinal bridge areas

clean with no crushed or pulverized material and no evidence of shear displacement. These surface characteristics indicated that tensile stresses were responsible for the initiation and propagation of the wing cracks. Also the characteristics of the failure surface in the middle region were investigated. There was a significant amount of pulverized and crushed gypsum and traces of shear displacement, indicated that a shearing failure had taken place. It is to be note that, when $EJC=0.6$ this coalescence appears in samples consisting one, two and three bridge areas.

Type III-Coalescence with two shear cracks

Coalescence with shear cracks, as defined in Fig. 7c, f and i, occurs when $EJC=0.4$. The mechanism of failure was characterized first by initiation of wing cracks followed by the initiation of secondary cracks at the tips of the joint segments. Then the two wing cracks were stopped while the two secondary cracks were propagated to meet each other at a point in the bridge area. The propagation and coalescence of the secondary cracks brought bridge areas to failure. The shear failure surface is in a wavy mode. Inspection of the surface of the cracks producing coalescence reveals the presence of many small kink steps, crushed gypsum and gypsum powder, which suggested coalescence through shearing. It is to be note that, when $EJC=0.4$, this coalescence appears in samples consisting one, two and three bridge areas.

3.2 The failure mode in the bridge areas under high normal stress (8 MPa)

Type II: Coalescence with mixed crack (shear/tensile)

This coalescence, as defined in Fig. 8a, d and g, occurred when EJC=0.8. At first the wing cracks were initiated at the tip of the joints and propagated stably. Afterward these wing cracks connect to each other by a shear crack.

Examining the failure surface in near the joint tips, it was noticed that there was smooth and clean with no crushed or pulverized material and no evidence of shear displacement. These surface characteristics indicated that tensile stresses were responsible for the initiation and propagation of the wing cracks.

Also the characteristics of the failure surface in the middle region were investigated. There was a significant amount of pulverized and crushed gypsum and traces of shear displacement, indicated that a shearing failure had taken place. It is to be note that, when EJC=0.8 this coalescence appears in samples consisting one, two and three bridge areas. By comparison of Fig. 7 and Fig. 8 for EJC=0.8, it can be found that the tensile failure mode change to mixed failure mode with increasing in the normal stress.

Type III-Coalescence with two shear cracks

Coalescence with shear cracks, as defined in Fig. 8 b, c, e, f, h and i, occurs when EJC \leq 0.6. The mechanism of failure was characterized first by initiation of wing cracks followed by the initiation of secondary cracks at the tips of the joint segments. Then the two wing cracks stopped while the two secondary cracks propagated to meet each other at a point in the bridge between the two inner tips of the preexisting joints. The propagation and coalescence of the secondary cracks brought bridge areas to failure. The shear failure surface is in a wavy mode. Inspection of the surface of the cracks producing coalescence reveals the presence of many small kink steps, crushed gypsum and gypsum powder, which suggested coalescence through shearing. It is to be note that, when EJC \leq 0.6, this coalescence appears in samples consisting one, two and three latitudinal bridges.

4. Description of the failure modes

The failure mode correlates quite well with the continuity of the joints and rock bridges, which can be described by the “effective joint coefficient”.

Type I: The oval mode coalescence with two wing cracks

For the bridge areas with the EJC=0.8 under low normal stress (1 MPa), there is very large extension of joint surface in front of the bridge tips (Table 2) and distance between the tip of the joints is short. Therefore a very high stress concentration (tensile and shear) is established due to the interaction between the joint tips. The tensile strength of the material existing at the tip of the joints is less than the shear strength and tensile stress intensity at tips of the joints is strong enough to produce the small tensile cracks tending to split the bridge area. Since, the tensile stress intensity is not enough to cause unstable crack growth therefore an increase in external load is necessary to elongate the existing tensile cracks. After the wing crack has grown enough, the contribution of the wing opening to the stress field redistribution becomes significant. In this time, the crack-generated tensile stress field and the effect of interaction between the crack tip and opposite joint tip (that are indeed situated very close to each other) is so strong that tend to unstable wing cracks growth connecting the joints. Since no new fracture produces in the midst zone, the coalescence left an oval core of intact material completely separated from the sample

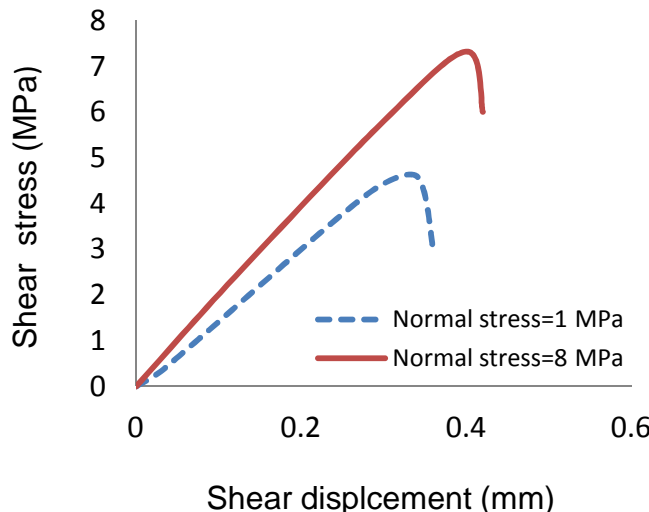


Fig. 9 Shear stress versus shear displacement curves for the models which are under two different normal stresses

(Fig. 7

Type III: Coalescence with mixed crack (shear/tensile)

This coalescence occurs when EJC=0.6 under low normal stress (1MPa) ((Fig. 7b, e and h) and EJC=0.8 under high normal stress (3.8MPa) (Fig. 8a, d and g). According to the characteristic of the failure surface, it seems that at first high tensile stresses concentration reaches to tensile strength of material existing at the tips of the joints and wing cracks initiate. The tensile strength of material is less than its shear strength so before the shear stresses concentration could overcome to shear strength, the tensile stress concentration reach to critical value and wing cracks initiate at tips of the joints. Afterward the wing cracks stopped suggesting that the tensile stresses were eliminated at the wing cracks. With increasing external loading, the shear stresses concentration at tips of the wing cracks reaches to critical value and the newborn shear cracks is created at tips of the wing cracks. These shear cracks propagate till bring the bridge area to failure.

Type IV: Coalescence with two shear cracks

This coalescence occurs when EJC=0.4 (Table 2) under low normal stress (1MPa) ((Fig. 7c, f and i) and EJC≤0.6 under high normal stress (3.8MPa) ((Fig. 8 b, c, e, f, h and i)). In this case the high stress concentration (tensile and shear stresses) is established at tips of the joints due to high external loading. At first, the tensile stresses reach to critical value (because the tensile strength of the material existing at the tip of the joints is less than its shear strength) and two wing cracks initiated at the tips of the joints. The tensile stresses was released due to wing cracks initiated at the tips of the joints so two wing cracks were stopped. With increasing in external loading, the tensile stress concentration at tips of the wing cracks reach to critical value again and tensile cracks can propagate for a short distance in a curvilinear path. Before the wing cracks could propagate further, the shear stress concentration leads to the secondary cracks initiation at the tips of the preexisting joints. The external shear loading must be increased that cause the shear stresses concentration at tips of the shear cracks overcome to shear strength of material. This shear cracks propagate till the end of the test. The propagation and coalescence of the secondary cracks brought bridge areas to failure in a wavy mode.

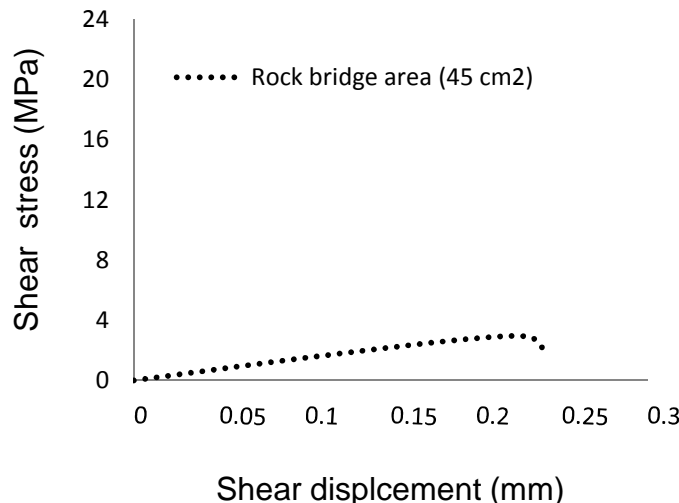


Fig. 10 Shear stress versus shear displacement curves for three models which have three different areas of bridge.

It is to be note that increasing in the normal stress changes the tensile failure to shear failure mode in bridges.

5. Description of the curves of shear stress versus shear displacement

5.1 The effect of normal stress on the shear stress versus shear displacement curve

Fig. 9 shows the shear stress versus shear displacement curves for the models which are under two different normal stresses, i.e. 1 MPa and 3.8 MPa. The models consist of one bridge. The area of rock bridges was 90 cm^2 . The inclination of the curve, or shear stiffness of bridge, was increased with increasing the normal stress. In fact the interlocking force between the grains was increased due to increasing in normal stress. This leads to increasing in the shear stiffness of bridge.

Also the peak shear strength of bridge was increased with increasing the normal stress due to increasing in interlocking force.

5.2 The effect of rock bridge area on the shear stress versus shear displacement curve

Fig. 10 shows shear stress versus shear displacement curves for three models which have three different areas of bridge, i.e. 45 cm^2 , 90 cm^2 and 145 cm^2 . Also the shear curve of intact model has been shown in this figure. The jointed models were consisted of one bridge. All models were subjected to 3.8 MPa of normal stress.

The intact model has the highest shear stiffness (inclination of the curve) but its stiffness was decreased with appearance of the joint in the model. The more the joint expansion is, the higher the stress concentration at the joint tips is. The higher the stress concentration is, the weaker the

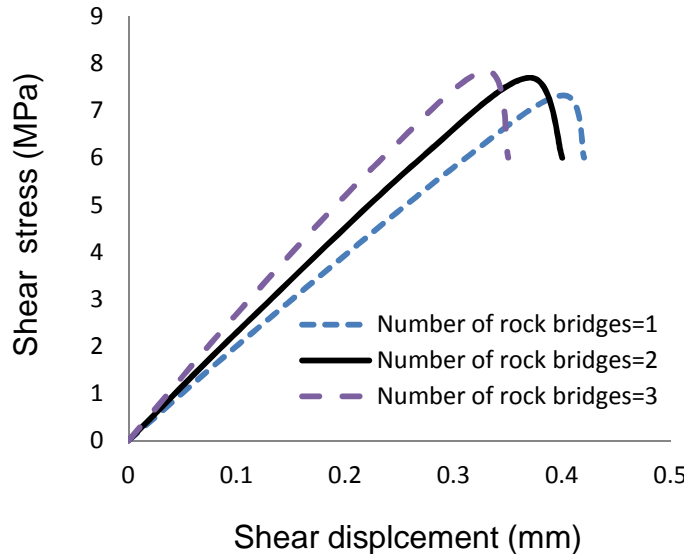


Fig. 11 Shear stress versus shear displacement curves for three models which have three different number of bridge area

shear bond is. Whereas the shear stiffness is related to the strength of shear bonds, therefore it can be concluded that the shear stiffness is decreased with decreasing the bridge area. Also the peak shear strength of bridge was increased with increasing the bridge area.

5.3 The effect of number of bridge area on the shear stress versus shear displacement curve

Fig. 11 shows shear stress versus shear displacement curves for three models which have three different number of bridge, i.e. one, two and three number. The bridge areas were occupied 90 cm^2 of total shear surface and were subjected to 3.8 MPa of normal stress.

The inclination of the curve, or shear stiffness of bridge, was increased slightly with increasing the bridge number.

With increasing the number of bridge area the number of surrounded joint increase while the joint length is constant. Whereas the stress concentration at tip of the surrounded joint is less than that at tip of the edge joint therefore the concentrated stress in the model was increased with decreasing the bridge number; because the number of surrounded joint was decreased. The more the stress concentration is, the weaker the shear bond is. It means that the shear stiffness was decreased with decreasing the bridge number.

Also the peak shear strength of bridge was increased with increasing the bridge number. The increasing in shear resistance can be explained by the Fracture Mechanics Theory, which indicates that for surrounded crack the Stress Intensity Factors (K_I and K_{II}) is less than edge crack at equal cracks length. This leads to higher bridge resistance. In fact with increasing in the number of bridge the number of surrounded crack increases while the crack length is constant. Therefore the Stress Intensity Factor decrease at tips of the joints and consequently the shear resistance increase dramatically.

6. Conclusion

The shear behavior of rock-like specimens containing various number of bridge areas with different areas has been investigated under two different normal loads through direct shear test. The results show that both of the failure pattern and failure mechanism are mostly influenced by EJC and normal stress. While both of the shear strength and shear stiffness are closely related to the ratio of bridge surface to total shear surface, number of bridge and normal stress. The following conclusions can be drawn from the experimental tests

1. In the fixed area of the bridge under fixed normal stress, with the increase in the effective joint Coefficient, a very high stress concentration (tensile and shear stress) is established at tip of the joints due to the interaction between the joint tips.
2. Under the low normal stress, the shear failure mode in the bridge changes to the tensile failure mode by increasing in the effective joint Coefficient.
3. Under the high normal stress, the shear failure mode in the bridge changes to the mixed failure mode by increasing in the effective joint Coefficient.
4. The shear strength is closely related to the bridge area failure pattern and failure mechanism, so that in the fixed area of the bridge under fixed normal stress, the bridge resistance reduced with change in failure mode from shear to tensile.
5. For the fixed area of the rock bridge, the shear resistance along the failure surface increase with increasing in the number of bridge area.

References

- Ayatollahi, M.R. and Sistaninia, M. (2011), "Mode II fracture study of rocks using Brazilian disk specimens", *Int. J. Rock Mech. Min. Sci.*, **48**(5), 819-826.
- ASTM (1971), *Standard method of test for splitting tensile resistance of cylindrical concrete specimens*, ASTM designation C496-71.
- ASTM (1986), *Test method for unconfined compressive resistance of intact rock core specimens*, ASTM designation D2938-86.
- Barragan, B., Gettu, R., Agullo, L. and Zerbino, R. (2006), "Shear failure of steel fiber-reinforced concrete based on push-off tests", *ACI Mater. J.*, **103**(4), 251-257.
- Bobet, A. and Einstein, H.H. (1998), "Fracture coalescence in rock-type materials under uniaxial and biaxial compression", *Int. J. Rock Mech. Min. Sci.*, **35**(7), 863-888.
- Eberhardt, E., Kaiser, P.K. and Stead, D. (2002), "Numerical analysis of progressive failure in natural rock slopes", *ISRM International Symposium-EUROCK 2002, International Society for Rock Mechanics*.
- Dai, F., Xia, K., Zheng, H. and Wang, Y.X. (2011), "Determination of dynamic rock mode-I fracture parameters using cracked chevron notched semi-circular bend specimen", *Eng. Fract. Mech.*, **78**(15), 2633-2644.
- Einstein, H.H., Veneziano, D., Baecher, G.B. and O'reilly, K.J. (1983), "The effect of discontinuity persistence on rock slope stability", *Proceedings of the International journal of rock mechanics and mining sciences & geomechanics abstracts.*, **20**(5), 227-236, Pergamon.
- Gehle, C. and Kutter, H.K. (2003), "Breakage and shear behaviour of intermittent rock joints", *Int. J. Rock Mech. Min. Sci.*, **40**(5), 687-700.
- Ghazvinian, A., Nikudel, M.R. and Sarfarazi, V. (2007), "Effect of rock bridge continuity and area on shear behavior of joints", *11th congress of the International Society for Rock Mechanics*, Lisbon, Portugal.
- Ghazvinian, A., Nikudel, M.R. and Sarfarazi, V. (2007), "Effect of rock bridge continuity and area on shear behavior of joints", *Proceedings of the Second Half Century of Rock Mechanics, Three Volume Set: 11th Congress of the International Society for Rock Mechanics*, **1**, 247, CRC Press.

- Haeri, H. (2015), "Influence of the inclined edge notches on the shear-fracture behavior in edge-notched beam specimens", *Comput. Concrete*, **16**(4), 605-623.
- Janeiro, R.P. and Einstein, H.H. (2010), "Experimental study of the cracking behavior of specimens containing inclusions (under uniaxial compression)", *Int. J. Fract.*, **164**(1), 83-102.
- Jiang, Z., Wan, S., Zhong, Z., Li, M. and Shen, K. (2014), "Determination of mode-I fracture toughness and non-uniformity for GFRP double cantilever beam specimens with an adhesive layer", *Eng. Fract. Mech.*, **128**, 139-156.
- Lancaster, I.M., Khalid, H.A. and Kougioumtzoglou, I.A. (2013), "Extended FEM modelling of crack propagation using the semi-circular bending test", *Constr. Build. Mater.*, **48**, 270-277.
- Li, Y.P., Chen L.Z. and Wang Y.H. (2005), "Experimental research on pre-Cracked marble", *Int. J. Solid. Struct.*, **42**, 2505-2016.
- Mughieda, O.S. and Khawaldeh, I. (2004), "Scale effect on engineering properties of open non-persistent rock joints under uniaxial loading", *Bölgesel Kaya Mekaniği Sempozyumu/ROCKMEC'2004-VIIth Regional Rock Mechanics Symposium*, Sivas, Türkiye.
- Mughieda, O.S. and Khawaldeh, I. (2006), "Coalescence of offset rock joints under biaxial loading", *Geotech. Geol. Eng.*, **24**(4), 985-999.
- Noël, M. and Soudki, K. (2014), "Estimation of the crack width and deformation of FRP-reinforced concrete flexural members with and without transverse shear reinforcement", *Eng. Struct.*, **59**, 393-398.
- Ozcebe, G., Ersoy, U. and Tankut, T. (1999), "Minimum flexural reinforcement for T-beams made of higher strength concrete", *Can. J. Civil Eng.*, **26**(5), 525-534.
- Sagong, M. and Bobet, A. (2002), "Coalescence of multiple flaws in a rock-model material in uniaxial compression", *Int. J. Rock Mech. Min. Sci.*, **39**(2), 229-241.
- Shen, B. (1995), "The mechanism of fracture coalescence in compression-experimental study and numerical simulation", *Eng. Fract. Mech.*, **51**(1), 73-85.
- Shen, B., Stephansson, O., Einstein, H.H. and Ghahreman, B. (1995), "Coalescence of fractures under shear stresses in experiments", *J. Geophys. Res.-all series*, **100**, 5975-5975.
- Takeuchi, K. (1991), "Mixed-mode fracture initiation in granular brittle materials", M.S. Thesis, Massachusetts Institute of Technology, Cambridge.
- Wang, Q.Z., Feng, F., Ni, M. and Gou, X.P. (2011), "Measurement of mode I and mode II rock dynamic fracture toughness with cracked straight through flattened Brazilian disc impacted by split Hopkinson pressure bar", *Eng. Fract. Mech.*, **78**(12), 2455-2469.
- Wang, Q.Z., Gou, X.P., Fan, H. (2012), "The minimum dimensionless stress intensity factor and its upper bound for CCNBD fracture toughness specimen analyzed with straight through crack assumption", *Eng. Fract. Mech.*, **82**, 1-8.
- Wang, T., Dai, J.G., Zheng, J.J. (2015), "Multi-angle truss model for predicting the shear deformation of RC beams with low span-effective depth ratios", *Eng. Struct.*, **91**, 85-95.
- Wong, R.H.C., Chau, K.T., Tang, C.A. and Lin, P. (2001), "Analysis of crack coalescence in rock-like materials containing three flaws-Part I: experimental approach", *Int. J. Rock Mech. Min. Sci.*, **38**(7), 909-924.
- Yoshihara, H. (2013), "Initiation and propagation fracture toughness of solid wood under the mixed Mode I/II condition examined by mixed-mode bending test", *Eng. Fract. Mech.*, **104**, 1-15.